

Self-Assembly of Styryl Naphthalene Amphiphiles in Aqueous Dispersions and Interfacial Films: Aggregate Structure, Assembly Properties, Photochemistry, and Photophysics

Liaohai Chen,[†] Cristina Geiger,[‡] Jerry Perlstein,[‡] and David G. Whitten^{*†}

Chemical Science and Technology Division, Los Alamos National Laboratory, Los Alamos, New Mexico 87545, and Department of Chemistry and NSF Center for Photoinduced Charge Transfer, University of Rochester, Rochester, New York 14627

Received: March 11, 1999; In Final Form: May 23, 1999

A study of phospholipid and fatty acid amphiphiles containing the isomeric *trans*- α - and β -styrylnaphthalene chromophores is reported. On the basis of simulations for Langmuir films of fatty acids terminated with the two chromophores, it was anticipated that the β -styrylnaphthalene fatty acids should be able to pack into compact layers, having an extended glide or herringbone arrangement similar to those observed for corresponding stilbene, tolan, or azobenzene amphiphiles. In contrast, the simulations suggested that such an arrangement might be precluded on steric grounds for the isomeric α -styrylnaphthalene derivatives. The experimental studies carried out indicate that the β -styrylnaphthalene fatty acids and phospholipids do in fact exhibit assembly properties and photophysical behavior similar to that observed for the stilbene and tolan amphiphiles; thus we find evidence for aggregates having similar “signatures” to those observed previously for both films at the air–water interface and aqueous suspensions. The behavior of the α -styrylnaphthalene amphiphiles is much more complex. Whereas aqueous dispersions of the phospholipid and highly compressed films at the air–water interface suggest the presence of weak aggregates (possibly dimers) having a translation or face-to-face structure, studies of the fatty acid derivative at the air–water interface suggest that the α fatty acid may form a “pinwheel” or herringbone cluster before compression such that drastically different photochemistry and photophysics is observed as a function of compression.

Introduction

In several recent studies we have shown that incorporation of an aromatic group into the hydrocarbon chain of an amphiphile such as a fatty acid or phospholipid results in enhanced, and in some cases unusual, self-assembly processes, as a consequence of strong noncovalent attraction between the aromatic chromophores.^{1–4} These interactions are manifested by changes in the absorption spectra, photophysics and photochemistry of the aromatic chromophore, as well as by changes in the structures or properties of the resulting assembly. In several cases, for example for *trans*-stilbene derivatives,^{5–7} simple phenyl, biphenyl, and terphenyl derivatives,⁸ azobenzenes,^{9,10} tolans,^{11,12} and α , ω -diphenylpolyenes,¹³ indications are strong that for both the “unit aggregate” and the extended array in films and aqueous dispersions, the nearest neighbors show an edge-to-face arrangement, which leads to an extended glide or herringbone array. However, in other cases, most notably the apparently structurally similar styrene and styrylthiophene amphiphiles,^{14,15} there is good evidence through experimental observations such as novel photoreactivity in the aggregates and simulations that the preferred structures may result from face-to-face interactions between neighboring aromatic chromophores, resulting in an extended translation layer array.

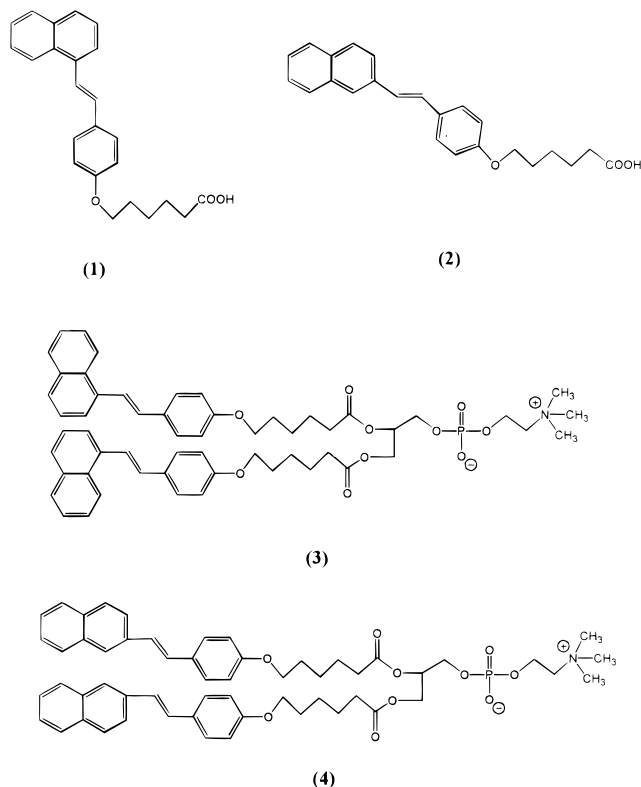
In an effort to probe the relative importance of different factors that may control the self-assembly of aromatic amphiphiles, we considered the styrylnaphthalene chromophore as potentially interesting for fruitful investigation because of the existence of two isomeric chromophores having similar absorp-

tion spectra and photophysics for the monomer, yet very different shape and potentially different possibilities for packing in organized assemblies because of the nature geometry different substitute position in the aromatic rings.¹⁶ In previous studies it has been shown that *trans* isomers of simple styrylnaphthalene derivatives exhibit similar photophysical behavior for the α - and β -isomers and photoisomerization behavior not very different from that of *trans*-stilbene.¹⁷ From simple modeling considerations we recognized that amphiphiles constructed by attaching a fatty acid chain to the para position of the phenyl ring of α - and β -*trans*-styrylnaphthalene should result in molecules having very different shapes. Thus the β -isomer would be anticipated to exist preferentially in the glide configuration in films and vesicles; as an “elongated” configuration it might be anticipated to be very similar to the corresponding stilbene and azobenzene amphiphiles such that edge-to-face interactions should be easily attained and hence favored. In contrast, the α -isomer would be anticipated to have a bent shape in the “extended” amphiphile such that it would be expected to fairly easily pack in a translation layer structure, permitting face-to-face interactions, whereas an edge-to-face arrangement resulting in an extended glide or herringbone lattice should be unfavorable because of the shape or steric effects.

In the current paper we report a study of the self-assembly and aggregation behavior of fatty acid and phospholipid derivatives containing the styrylnaphthalene chromophore (Scheme 1). The synthesis of fatty acid derivatives **1** and **2** were accomplished by techniques similar to those used for other aromatic amphiphiles and from these the corresponding phospholipids **3** and **4** were obtained.⁸ We have interrogated the behavior of **1** and **2** in films at the air–water interface and in supported multilayers by Langmuir–Blodgett technique and also

[†] Los Alamos National Laboratory.

[‡] University of Rochester.

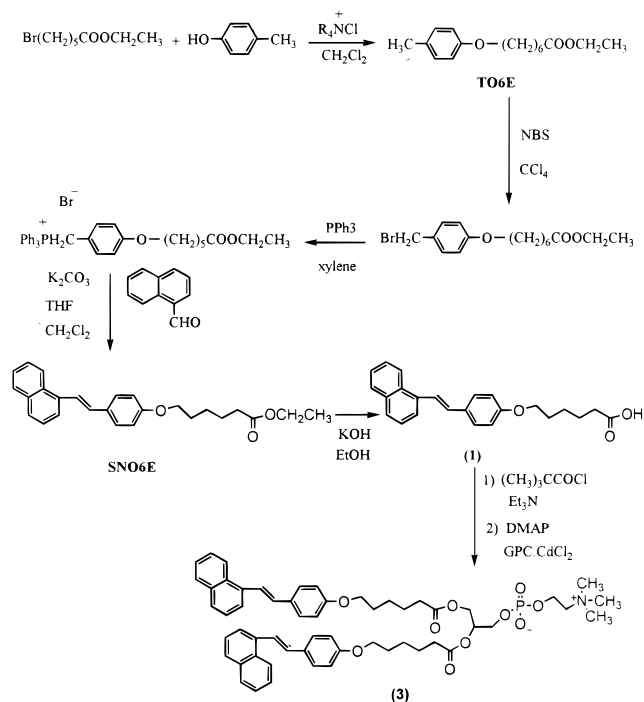
SCHEME 1: Chemical Structures for Compounds Used in This Study


examined aqueous dispersions of the phospholipids **3** and **4**. Results of these investigations indicate markedly different self-assembly and aggregation behavior for the two styrylnaphthalene isomers. As anticipated from the above discussion the two amphiphiles incorporating a β -styrylnaphthalene chromophore exhibit aggregation very similar to that found for the stilbenes and related aromatics. The behavior of the α -styrylnaphthalene amphiphiles is, in contrast, much more complex and provides a remarkable demonstration of the role of competing interactions in the self-assembly process and in resultant assembly properties.

Experimental Section

Reagents were purchased from Aldrich and were used as received. All solvents for spectroscopic studies were spectroscopic grade either from Aldrich or Fisher. Milli-Q water, obtained by passing house-deionized water through a Millipore-RO/UF water purification system, was used for all measurements in an aqueous medium. L- α -Glycerophosphorylcholine as the cadmium chloride complex, lipophilic Sephadex LH-20 (25–100- μ m beads), Sephadex G-50, and L- α -dimyristoylphosphatidylcholine (DMPC, 99+%) were purchased from Sigma Chemical Co.

The α -styrylnaphthalene fatty acid derivative (**1**) was synthesized in a multistep synthesis depicted in Scheme 2. A mixture of 450 mL of methylene chloride, 450 mL of water, ethyl 6-bromohexanoate (40.0 g, 0.179 mol), *p*-cresol (9.68 g, 0.09 mol), sodium hydroxide (5.38 g, 0.13 mol), and quaternary ammonium bromide (17.34 g, 0.05 mol) was stirred vigorously at room temperature for 12 h. After working up, the crude product was purified by vacuum distillation and 14.75 g (66% yield) of pure product (TO6E) was obtained at 117–120 °C (0.6 mmHg). Bromination of TO6E with NBS in carbon tetrachloride afforded the bromo derivative in a 69% yield. The styrylnaphthalene chromophore was synthesized by the Wittig

SCHEME 2: Synthesis Route for 1 and 3


reaction between 1-naphthaldehyde and the corresponding Wittig salt. Thus, dry bromoester (2.8 g, 8.5 mmol) and triphenylphosphine (3.3 g, 12.6 mmol) were dissolved in the dry xylene under the nitrogen. The reaction mixture was refluxed overnight and the resulting Wittig salt was filtered, recrystallized with chloroform/benzene, and dried in a vacuum desiccator for 12 h. It was then dissolved (1.5 g, 2.52 mmol) in 50 mL of dry, freshly distilled tetrahydrofuran (THF) and 40 mL of methylene chloride, followed by the addition of K_2CO_3 (1.74 g, 12.6 mmol) and 10 mg of 18-crown-6. After the mixture was stirred for a few minutes, 1-naphthaldehyde (0.86 g, 5.54 mmol) was added slowly. The reaction mixture was then refluxed overnight. The crude product was purified by silica gel column chromatography using hexane/ethyl acetate (10%) as eluent to yield 0.91 g (90% yield) SNO6E, which was further purified by recrystallization from THF/hexane as white crystals. Hydrolysis of this ester in KOH/ethanol afforded the α -styrylnaphthalene fatty acid (**1**) in a 70% yield. 1H NMR ($CDCl_3$) δ : 8.3–6.9 (m, 13H); 4.0 (t, 2H); 2.4 (t, 2H); 1.85 (m, 2H); 1.75 (m, 2H); 1.55 (m, 2H). Elemental Analysis: calculated for $C_{24}H_{24}O_3$, C 79.97, H 6.71; found, C 80.23, H 6.66.

The corresponding phospholipid derivative (**3**) was prepared according to the routes previously described in the literature.⁸ 1H NMR ($CDCl_3$) δ : 8.2–6.8 (m, 24H); 7.06–7.02 (d, 2H); 5.2 (m, 1H); 4.4–3.7 (m, 10H); 3.4–3.3 (s, 9H); 2.4 (t, 4H); 1.85 (m, 4H); 1.75 (m, 4H); 1.55 (m, 4H). FAB: $C_{56}H_{64}NO_{10}P$ m/z calcd for ($M + H$) = 942.4, found 942.4.

The β -styrylnaphthalene fatty acid and its corresponding phospholipid derivative were synthesized on the basis of very similar procedures to those for the α -styrylnaphthalene derivatives but starting with a 2-naphthaldehyde. β -Styrylnaphthalene fatty acid (**2**): 1H NMR ($CDCl_3$) δ : 7.7–6.8 (m, 13H); 4.0 (t, 2H); 2.4–2.3 (t, 2H); 1.75 (m, 2H); 1.64 (m, 2H); 1.44 (m, 2H). Elemental Analysis: calculated for $C_{24}H_{24}O_3$, C 79.97, H 6.71; found, C 79.78, H 6.57. The β -styrylnaphthalene phospholipid (**4**): 1H NMR ($CDCl_3$) δ : 8.0–6.8 (m, 24H); 7.15–7.02 (d, 2H); 5.2 (m, 1H); 4.0–3.4 (m, 10H); 3.2 (s, 9H); 2.4 (t, 4H); 1.80 (m, 4H); 1.70 (m, 4H); 1.55 (m, 4H). FAB: $C_{56}H_{64}NO_{10}P$ m/z calcd for ($M + H$) = 942.4, found 942.4.

Absorption spectra were recorded on a Hewlett–Packard 8452A diode array spectrophotometer. Steady-state fluorescence was measured using a SPEX Fluorolog spectrofluorometer. All emission and excitation spectra were corrected for instrumental response. The irradiation of the samples was carried out at room temperature with a 200-W high-pressure mercury lamp (Oriel model 68700) with a 7-60 Corning glass filter ($300 < \lambda < 400$ nm). The Langmuir–Blodgett films of **1** and **2** were prepared by spreading a chloroform solution of material (1×10^{-3} M) onto an aqueous surface containing cadmium chloride (3×10^{-4} M) buffered with 1×10^{-5} M NaHCO_3 (pH = 6.8) on a KSV 5000 Langmuir–Blodgett trough. The temperature of the trough was controlled by a water bath. The monolayers were transferred onto quartz substrates that were previously treated by piranha solution in a vertical deposition protocol. Bilayer vesicles of **2** and **4** with DMPC were prepared on the basis of the literature procedure,¹⁸ and an ultrasonic liquid processor sonicator, model XL2015, from Misonic Inc. was used for probe sonication. The crystal structures of **1** and **3** were obtained by mounting the single crystals, which were grown from THF/ CHCl_3 and methanol respectively, on a glass fiber under Paratone-8277 and immediately placed in a cold nitrogen stream at -80°C on the X-ray diffractometer. The X-ray intensity data were collected on a standard Siemens SMART CCD area detector system equipped with a normal focus molybdenum-target X-ray tube operated at 2.0 kW (50 kV, 40 mA). Monte Carlo simulated annealing experiments were carried out using PACK software¹⁹ to generate the details of the packing of the lowest-energy gas-phase monolayers for the fatty acid derivatives **1** and **3**. Molecular structures were generated using the CHEMX/CHEMLIB molecular modeling package.²⁰ Bond lengths and bond angles were optimized using the MM2 force field. All single-bond torsion angles were allowed to vary during the course of the simulation. Monolayers with either simple translation or glide layer symmetry were generated by the PACK routine. Approximately 700 low-energy monolayers were generated for each symmetry type for which surface area/molecule was computed to compare with the experimental results.

Results and Discussion

As shown in Figure 1 for the fatty acids, both styrylnaphthalene isomers show similar absorption spectra when dissolved at low concentrations (1×10^{-5} M) in organic solvents such as ethanol, acetonitrile, and chloroform, etc. under conditions where only the monomer should be present. Trans-to-cis photoisomerization of styrylnaphthalene derivative has been well studied in the literature,^{21–25} with an average measured quantum efficiency of 0.1. Thus, irradiation of either isomer in organic solvents under these conditions results in spectral changes consistent with photoisomerization to produce the corresponding cis isomers. This was confirmed by proton NMR studies in which the appearance of two set of the doublet peaks with chemical shifts of 6.54–6.52 ppm ($J = 8.7$) and 6.96–6.94 ppm ($J = 8.7$) was assigned to the alkene protons of the cis styrylnaphthalene isomer. The photoisomerization is reversible in the early phases for both the α - and β -fatty acids and appears to be qualitatively and quantitatively similar to the photoisomerization processes observed for the stilbenes and the simple styrylnaphthalene derivatives previously studied. For the *trans*- β -styrylnaphthalene fatty acid **2**, deposition of a film from a chloroform solution followed by compression results in a relatively sharp isotherm, very similar to those obtained from the corresponding *trans*-stilbene fatty acid derivatives or for saturated fatty acids such as arachidic acid. The limiting area

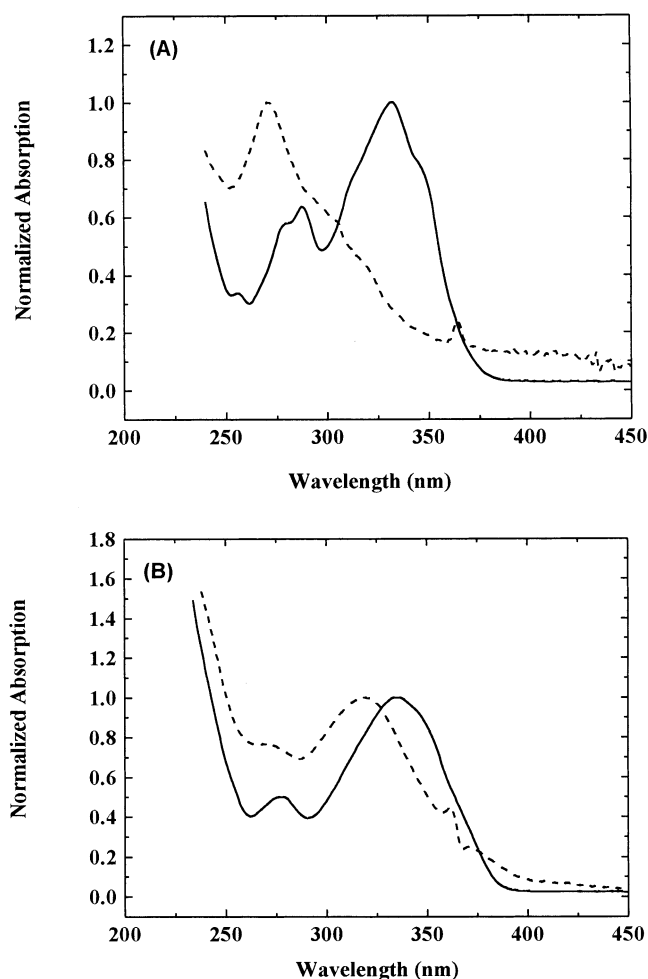


Figure 1. Normalized absorption spectra of **2** (A) and **1** (B) in different media. Solid line, in chloroform; dashed line, Langmuir–Blodgett monolayer film.

per molecule is 26.9 \AA^2 , which is also similar to that obtained for the corresponding *trans*-stilbene fatty acid. This area-per-molecule value derived from the isotherm is in good agreement with the one obtained from PACK simulation (26.7 \AA^2). The relatively small area per molecule is consistent with the styrylnaphthalene chromophore existing in an extended configuration in the films. The absorption spectrum for **2** in Langmuir–Blodgett multilayers transferred to quartz supports shows a pronounced blue shift (~ 70 nm) compared to solution as indicated in Figure 1A. Accordingly, the fluorescence spectrum also exhibits similar red shift, reminiscent of those obtained for the stilbene and azobenzene amphiphiles in LB films. In fact the shape and wavelength of the shifted absorption spectrum is remarkably similar to those for stilbene, tolan, and α,ω -diphenylpolyenes in the same assemblies, even though the absorption spectrum for the monomer is at relatively longer wavelengths. The corresponding phospholipid, **4**, forms clear dispersions upon sonication in aqueous solution. The absorption and fluorescence spectra of these dispersions are virtually identical to those of the LB films of **2**. Dilution of an aqueous dispersion of **4** with a dispersion containing an excess of the saturated phospholipid DMPC results in a shift to longer wavelengths. These dispersions are resistant to dilution as indicated by the finding that no changes can be detected in the absorption and emission spectra until the ratio of DMPC/ β -styrylnaphthalene reaches 36:1 (Figure 2A). It should be pointed out that the spectrum of the most diluted solutions is not the

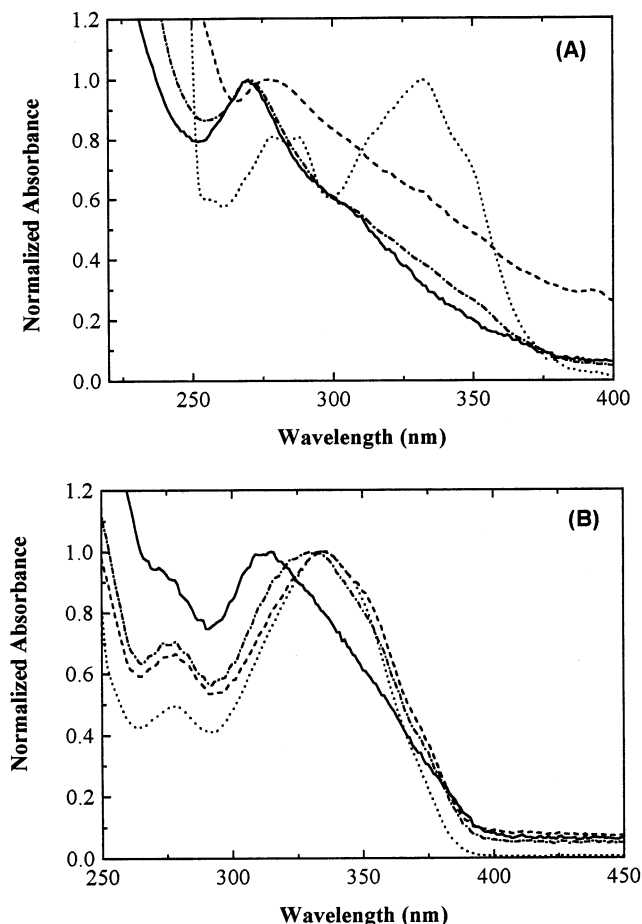


Figure 2. Normalized absorption spectra of **4** (A) and **2** (B) aqueous dispersion upon dilution by DMPC. (A) solid line, pure **4** aqueous dispersion; dash-dot line, DMPC:**4** = 5:1; dashed line, DMPC:**4** = 36:1; dotted line, in chloroform. (B) Solid line, pure **2** aqueous dispersion; dash-dot line, DMPC:**2** = 5:1; dashed line, DMPC:**2** = 20:1; dotted line, in chloroform.

same as the one in chloroform where only monomer is present; it is still blue-shifted compared to the monomer, but red-shifted compared to the original aggregated form, suggesting that an intermediate product may be formed with a smaller aggregation number relative to the aqueous dispersion of **4**. Even though both **2** and **4** undergo photoisomerization as the predominant photoreaction when irradiated in dilute solutions as the monomer, the LB films of **2** and the aqueous dispersions of **4** show little change upon irradiation at 300–400 nm. The photostability of **2** and **4** in films and aqueous bilayer assemblies, respectively, as well as the pronounced spectral shifts suggest that the arrangement of the fatty acid **2** in LB films and of the phospholipid **4** in aqueous dispersions is very similar to that of the stilbene and azobenzene amphiphiles in corresponding media.⁴ Thus the observed behavior is consistent with self-assembly of these amphiphiles to form similar aggregates, most likely with an extended glide or herringbone structure in which the primary interaction is an edge-to-face interaction between neighboring aromatics. In these arrangements both photoisomerization and photodimerization from β -styrylnaphthalene chromophores are precluded.

For the α -styrylnaphthalene amphiphiles quite different behavior is observed. When the fatty acid **1** is compressed to a pressure of 35 mN/m, a film with a limiting area of 24 Å² is obtained, which is again very similar to the value obtained from PACK simulations. Not surprisingly, after the film was trans-

ferred to a quartz support, the absorption spectrum of this film (Figure 1B) is quite different from that of **2**, showing only a small blue shift of 18 nm compared with the solution spectrum, whereas the fluorescence shows a small red shift. Similar absorption and fluorescence spectra are also observed for sonicated aqueous dispersions of **3**. In contrast to the results for the β -styrylnaphthalene derivatives, dilution of an aqueous dispersion of **3** with a dispersion containing an excess as small as five-fold of the saturated phospholipid DMPC results in a shift to longer wavelengths closely corresponding to the monomer of the α -styrylnaphthalene (Figure 2B), suggesting that the aggregates of **3** may be much less stable than those of **4** or the corresponding stilbene phospholipids. Irradiation of films of **1**, prepared by compression to 20 mN/m and transferred to quartz slides, or aqueous dispersions of **3** with light in the range 300–400 nm results in a clean bleaching of the long-wavelength transition in each case. In contrast to the photoisomerization of the monomer in solution, the bleaching observed here is not reversed by short-wavelength irradiation, and the spectral shape is also quite different from that for photoisomerization. The photoproduct of irradiated aqueous dispersions of α -styrylnaphthalene phospholipid was tentatively identified by NMR analysis. Thus, the aqueous dispersions of **3** was irradiated with 300 nm wavelength light in a Rayonet photochemical reactor for a period of 18 h, and the resulting solution was hydrolyzed and then extracted with chloroform. Because of the poor solubility of **3** in the aqueous solution, only a small amount of photoproduct was isolated. A relatively noisy NMR spectrum for the photoproduct was obtained, yet there was a distinguishable new peak appearing at 3.6 ppm. Because the chemical shift for cyclobutane protons is usually between 3.3 ppm and 3.7 ppm, and no protons from the styrylnaphthalene phospholipid have a peak in this region, the signal maybe most reasonably assigned to the protons associated with the cyclobutane hydrogens for the corresponding styrylnaphthalene photodimers. Thus we may tentatively assign the photoproduct to a dimer formed by the cycloaddition of two α -styrylnaphthalene units. On the basis of the photoreactivity as well as the spectral shift, it seems reasonable that both assemblies of the α -styrylnaphthalene amphiphiles pack into transition layer structures where photodimerization is topologically allowed.

The contrast in behavior between α -isomers **1** and **3** and β -isomers **2** and **4** upon self-assembly is consistent with different aggregation behavior or different extended structures for the two types of amphiphiles. On the basis of their spectral similarities, previously obtained crystal structure data for the stilbenes, and the lack of photoisomerization or photodimerization (despite reasonably long fluorescent lifetimes), it is reasonable to assign a herringbone or glide structure with edge-to-face interactions between neighbors to the β -styrylnaphthalene amphiphiles. In fact, from the remarkable spectral similarity of aggregates formed from the stilbenes, tolans, α,ω -diphenylpolyenes, and now β -styrylnaphthalenes, it appears that we can associate this type of aggregate with a characteristic large spectral shift and "signature" as shown in Figure 1. The smaller spectral blue shifts in absorption and apparent photodimerization for the α -styrylnaphthalene amphiphiles are similar to the previously observed behavior of styrylthiophenes and styrene derivatives and seem most consistently attributable to a translation layer structure extended array that is characterized by face-to-face interactions.

Additional support for these assignments may be obtained from the crystal structures of **1** and **2** (Figure 3). Single crystals of **1** and **2** were grown from THF/CHCl₃ and methanol,

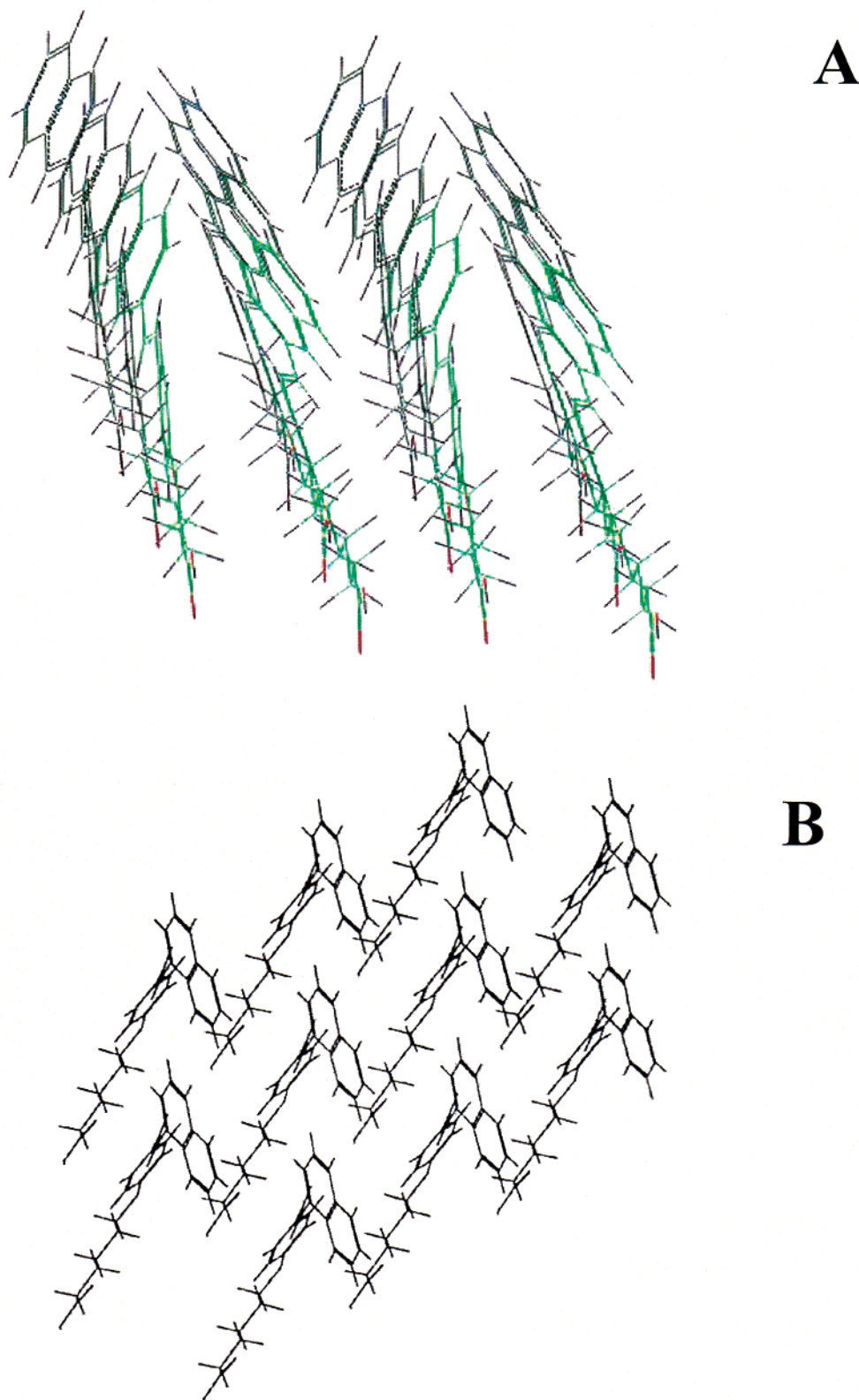


Figure 3. Single-crystal structures of **2** (A) and **1** (B).

respectively. As it has been found for several other aromatic-functionalized amphiphiles, we find that the crystals of **1** resemble an LB multilayer (γ -deposition) array. However, unlike the stilbenes, for **1** the styrylnaphthalene chromophores within a layer are in a face-to-face or translation array. Although there is clearly a face-to-face arrangement between neighboring

molecules, the separation between the olefin bonds of nearest neighbors is 7.7 Å, which is clearly greater than the “magic distance” required for a topologically controlled dimerization in the crystal. Not surprisingly, these crystals of **1** are photo-stable, unlike the compressed monolayer films or aqueous dispersions. For the crystals of **2**, the arrangement is also

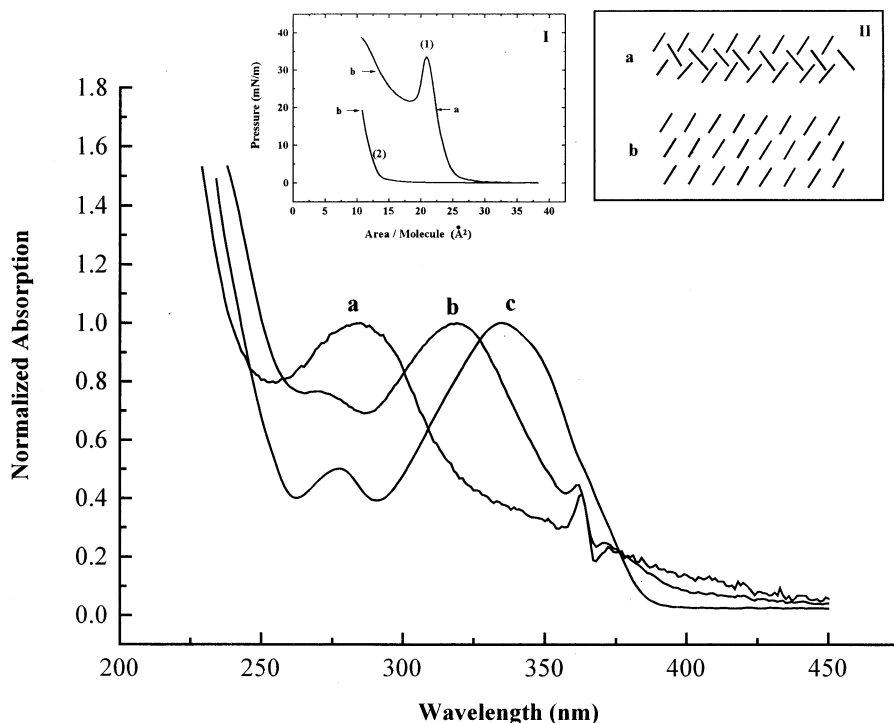


Figure 4. Normalized absorption spectra of LB films of **1** obtained at different compression stages: a, first compression; b, second compression; c, in chloroform. Inset I: Isotherms of **1** (1); first compression; (2); subsequent compression; inset II: schematic representation of chromophore orientation for **1**: a; glide or pinwheel aggregates; b; translation aggregates.

somewhat like an "LB multilayer arrangement"; however, here the extended molecules are tilted 68° from the layer normal, in contrast to the much closer to "perpendicular" arrangements found for the stilbene crystals and for **1**. Individual molecules are in the "extended" structure. It should be pointed out that the arrangement among molecules in the "layer" is a glide or herringbone arrangement; however, the edge-to-face interactions that occur between adjacent molecules in this structure are somewhat different from those observed for crystals of stilbene derivatives²⁶ or in simulations on the layer structures in that the closest approach is between phenyl rings of one molecule and a naphthyl group of its neighbor instead of the simple phenyl-phenyl contact that exists for the stilbene derivative.

Indications that the self-assembly of **1** may be much more complex than for other aromatic fatty acids examined thus far come from a study of its behavior in films at the air-water interface and the corresponding LB films obtained at different stages of compression. Thus when films of **1** are slowly compressed [Figure 4 I(1)], there is a sharp rise at a relatively large area/molecule, followed by a decrease in pressure after an early maximum of ca. 30–35 mN/m is reached and then a second increase. This "unusual" compression behavior is observed only on the initial compression. Decompression and subsequent recompression result in a single rise in the isotherm at much smaller areas per molecule [Figure 4 I (2)]. This behavior contrasts to that for the films of **2**, which exhibit constant isotherms with a single rise (no hysteresis) upon successive compression-decompression cycles. The films of **1** are stable enough to be transferred to quartz supports during the first rise in pressure, as well as during the second. Interestingly, the spectra of the LB films of **1** obtained during the two compression stages are quite different (Figure 4). The film of **1** obtained upon the second compression shows absorption and fluorescence spectra identical to those obtained for the aqueous dispersions as shown in Figure 1, which we have attributed to a translation layer arrangement. As described

above, these LB films are susceptible to rapid photobleaching. In contrast, the films of **1** obtained from the first compression show spectra nearly identical to those of **2**, which are characterized by a pronounced blue shift and the "signature" attributed to the "glide" or pinwheel aggregates above (Figure 4II). As would be anticipated for a glide aggregate with edge-to-face interactions, the films of **1** from this "first" compression are photostable.

The simplest interpretation of the observed behavior is that before to or during the first compression of **1** at the air-water interface, the molecules aggregate in small clusters or "unit aggregates" in which the favored noncovalent interactions are edge-to-face. As these clusters begin to pack together (first rise), an extended array or mosaic is formed, but the mismatch between the relatively small area occupied by the headgroups at the surface and the larger surface area of the pinwheel chromophore aggregates caused by the "bent" shape of the α -styrylnaphthalene renders this array metastable. Thus it collapses or rearranges to a more compact and stable translation layer array on further compression. To determine whether the interconversion of the two aggregates is reversible, we have examined the isotherms as a function of temperature. As shown in Figure 5, the collapse pressure for the first compression decreases as the temperature increases, suggesting a thermal instability of the edge-to-face arrays for α -styrylnaphthalenes. It also has been found that over a range of temperatures, once the "second" aggregate is formed, no return to the first is detected, reinforcing the idea that face-to-face interaction is the favored interaction for the bulky and "bent"-shape α -styrylnaphthalene chromophore in the amphiphile structures of **1** and **3**. The presence of two distinctly different aggregates in the films of **1** shows that the local and extended structure produced by self-assembly of functionalized amphiphiles may be strongly affected by competing forces or interactions. In this case favored noncovalent interactions control the local structure of small clusters but result in a metastable mosaic as the structure is

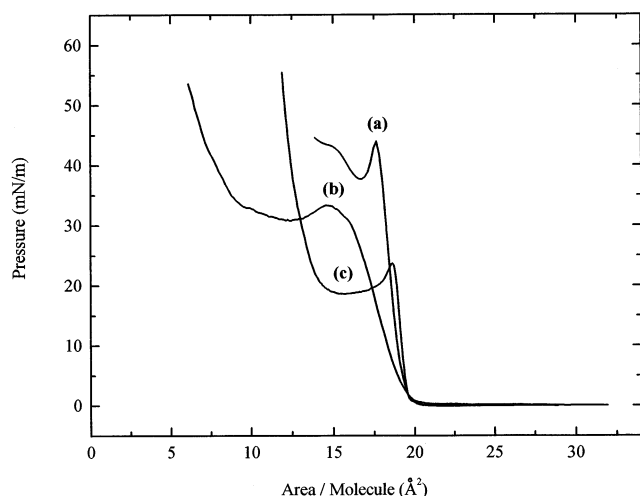


Figure 5. Isotherms of **1** in the different temperatures: (a) 5 °C, (b) 25 °C, and (c) 50 °C.

extended because of what appear to be unfavorable shape or packing interactions. This suggests exciting possibilities for designing new self-assembling systems that can generate synthetic membranes and related materials that may respond dramatically to small perturbations.

In summary, the behavior of α - and β -styrylnaphthalenes indicates again that noncovalent interaction between chromophores may play a key role in controlling self-assembly of functionalized amphiphiles. However, because face-to-face and edge-to-face interactions may be energetically quite similar, other considerations such as amphiphile geometry and packing may control the stable structures generated by self-assembly.

Acknowledgment. We are grateful to the Center for Material Science in Los Alamos National Laboratory, the US National Science Foundation (grant number CHE-9521048), and the Center for Photoinduced Charge Transfer for support of this research. We also thank Dr. Rene Lachicotte for help with X-ray measurements.

References and Notes

- (1) Nakahara, H.; Fukada, K.; Moebius, D.; Kuhn, H. *J. Phys. Chem.* **1986**, *90*, 6144–6148.
- (2) Evans, C. E.; Bohn, P. W. *J. Am. Chem. Soc.* **1993**, *115*, 3306–3311.
- (3) Whitten, D. G.; *Acc. Chem. Res.* **1993**, *26*, 502.
- (4) Whitten, D. G.; Chen, L.; Geiger, C.; Perlstein, J.; Song, X. *J. Phys. Chem.* **1998**, *102*, 10098.
- (5) Song, X.; Geiger, C.; Furman, I.; and Whitten, D. G. *J. Am. Chem. Soc.* **1994**, *116*, 4103.
- (6) Song, X.; Geiger, C.; Leinhos, U.; Perlstein, J.; Whitten, D. G. *J. Am. Chem. Soc.* **1994**, *116*, 10340.
- (7) Song, X.; Geiger, C.; Farahat, M.; Perlstein, J.; Whitten, D. G. *J. Am. Chem. Soc.* **1998**, *119*, 12481–91.
- (8) Geiger, C.; Perlstein, J.; Lachicotte, R.; Whitten, D. G. *Langmuir*, submitted.
- (9) Song, X.; Perlstein, J.; Whitten, D. G. *J. Am. Chem. Soc.* **1997**, *119*, 9144–9159.
- (10) Kremer, J. M. H.; Kops-Werkhoven, M. M.; Pathmamanoharan, C.; Gijzenman, O. L. J.; Wiersma, P. H. *Biochim. Biophys. Acta* **1977**, *471*, 177.
- (11) Furman, I.; Geiger, H. C.; Whitten, D. G.; Penner, T. L.; Ulman, A. *Langmuir*, **1994**, *10*, 837.
- (12) Farahat, C. W.; Penner, T. L.; Ulman, A.; Whitten, D. G. *J. Phys. Chem.* **1996**, *100*, 12616.
- (13) Spooner, S. P.; Ph.D. Dissertation, University of Rochester, 1993.
- (14) Zhao, X.; Perlstein, J.; Whitten, D. G. *J. Am. Chem. Soc.* **1994**, *116*, 10463.
- (15) Song, X.; Perlstein, J.; Whitten, D. G. *J. Phys. Chem.* **1998**, *102*, 5440.
- (16) Saltiel, J.; Choi, J.; Sears, D. F., Jr.; Eaker, D. W.; Mailory, F. B. *J. Phys. Chem.* **1994**, *98*, 13162.
- (17) Scoponi, M.; Gallinella, E.; Momicchioli, F. *J. Chem. Soc., Faraday Trans. 2* **1988**, *84*, 95.
- (18) Kuhn, H.; Mobius, D.; Bucher, H.; In *Physical Methods of Chemistry*; Weissberger, A.; Rossiter, B. W., Eds; Wiley: New York, 1972, Vol. 1, p 577.
- (19) Perlstein, J. *J. Am. Chem. Soc.* **1994**, *116*, 11420.
- (20) CHEMX is a molecular modeling program developed by Chemical Design Ltd.
- (21) Saltiel, J.; Tarkalanov, N.; Sears, D. F. Jr. *J. Am. Chem. Soc.* **1995**, *117*, 5586.
- (22) Gennari, G.; Cauzzo, G.; Galiuzzo, G.; Folini, M. *J. Photochem.* **1980**, *14*, 11.
- (23) Krysanov, S. A.; Alifimov, M. V. *Izv. Akad. Nauk SSSR, Ser. Fiz.* **1984**, *48*, 462.
- (24) Bartocci, G.; Masetti, F.; Mazzucato, U.; Marconi, G. *J. Chem. Soc., Faraday Trans. 2* **1984**, *80*, 1093.
- (25) Hammond, G.; Shim, S. C.; Van, S. P. *Mol. Photochem.* **1969**, *1*, 89.
- (26) Vaday, S.; Geiger, H. C.; Cleary, B.; Perlstein, J.; Whitten, D. G. *J. Phys. Chem.* **1997**, *101*, 321.